NASA TECHNICAL
MEMORANDUM

NASA TM X-3415

CASE FILE
COPY

NORMAL IMPINGEMENT OF A CIRCULAR
LIQUID JET ONTO A SCREEN IN
A WEIGHTLESS ENVIRONMENT

Eugene P. Symons

Lewis Research Center

Cleveland, Ohio 44135

NATIONAL AERONAUTICS AND SPACE ADMINISTRATION • WASHINGTON, D. C. • AUGUST 1976

1. Report No. NASA TM X-3415	2. Government Accession No.	3. Recipient's Catalog No.
4. Title and Subtitle NORMAL IMPINGEMENT OF A CIRCULAR LIQUID JET ONTO A SCREEN IN A WEIGHTLESS ENVIRONMENT		5. Report Date August 1976
		6. Performing Organization Code
7. Author(s) Eugene P. Symons		8. Performing Organization Report No. E-8710
9. Performing Organization Name and Address Lewis Research Center National Aeronautics and Space Administration Cleveland, Ohio 44135		10. Work Unit No. 506-21
		11. Contract or Grant No.
12. Sponsoring Agency Name and Address National Aeronautics and Space Administration Washington, D.C. 20546		13. Type of Report and Period Covered Technical Memorandum
		14. Sponsoring Agency Code

15. Supplementary Notes

16. Abstract

The normal impingement of a circular liquid jet onto a fine-mesh screen in a weightless environment was investigated. Equations were developed to predict the velocity of the emerging jet on the downstream side of the screen as a function of screen and liquid parameters and of the velocity of the impinging jet. Additionally, the stability of the emerging jet was found to be Weber number dependent. In general, excepting at high velocities, the screen behaved much as a baffle, deflecting the major portion of the impinging flow.

17. Key Words (Suggested by Author(s)) Weightlessness Screens Fluid jets Jet impingement	18. Distribution Statement Unclassified - unlimited STAR Category 34		
19. Security Classif. (of this report) Unclassified	20. Security Classif. (of this page) Unclassified	21. No. of Pages 30	22. Price* $4.00

NORMAL IMPINGEMENT OF A CIRCULAR LIQUID JET

ONTO A SCREEN IN A WEIGHTLESS ENVIRONMENT

by Eugene P. Symons

Lewis Research Center

SUMMARY

This report presents the results of an investigation of the normal impingement of a circular liquid jet onto a fine-mesh screen in a weightless environment. An approximate analytical evaluation of the phenomenon, based on the integral momentum theorem, was used in developing equations that were correlated with the experiment data to predict some facets of the gross liquid behavior following jet impingement on the screen surface. Generally, it was observed that the screen acted much as a baffle, deflecting the major portion of the impinging flow with the test liquids and screens employed. The emerging jet velocity on the downstream side of the screen was compared with the analytical predictions, and the stability of the emerging jet was found to be dependent on the Weber number.

INTRODUCTION

Recent studies have shown that capillary containment devices fabricated from fine-mesh screens and placed in spacecraft propellant tanks can provide a very effective means for the control and transfer of both cryogenic and earth-storable liquids in a reduced-gravity environment. For these devices to function properly, it is necessary that they either remain filled with liquid or are capable of being refilled.

In general, the devices can be thought to serve one of two purposes: (1) to provide liquid for engine restart capability or (2) to provide liquid for transfer under either zero or reduced gravitational conditions. In the typical engine restart application, the screen device is designed to retain a sufficient quantity of liquid to provide engine restart and then to be refilled by a settling of the bulk liquid due to the thrust imparted by the engine. In the typical transfer application, the screen device is designed to remain

filled and to maintain continuous contact with the bulk liquid throughout the transfer. However, upon liquid depletion, it may be desirable to refill the transfer device in a low-gravity environment for subsequent reuse (e.g., a serviceable satellite).

While there is little doubt that a carefully designed device for restart capability can be ultimately refilled because of the gravitational head provided by the engine's thrust, the time to accomplish refill can be greatly influenced by the amount of settled liquid that initially flows through the device. If most of the settled liquid is initially deflected by the screen, complete refill will not occur until the majority of the bulk liquid is settled.

In the case of refill of a transfer device, it is again important to understand the behavior of the incoming liquid as it contacts the screen surface. An optimum selection of the design and location of the inflow line will be influenced by the manner in which the incoming liquid interacts with the screen (i.e., the quantity of liquid passing through the screen) since the objective is the complete filling of the screen device.

To date there has been a considerable amount of effort expended in studying some of the basic characteristics of screen-liquid systems. Such things as bubble point, flowthrough pressure drop, parallel-flow pressure drop, screen wicking, vibration and transient pressure effects, and warm-gas pressurization effects on retention have been investigated. All of these relate to the capability of the capillary system to either retain liquid against some adverse gravitational head or to permit outflow from the screen device. Relatively little work has been done either experimentally or analytically to provide some fundamental understanding of liquid behavior during refill.

This report presents the results of a study to investigate the normal impingement of a circular liquid jet onto a simply supported screen surface in a weightless environment. The objective of the study was to examine the phenomenon in order to understand what criteria had to be met to cause the impinging liquid to flow through the screen. Additionally, some effort was directed toward determining what percentage of the impinging liquid was deflected by the screen surface and what percentage passed through the screen. As a part of the study, equations were developed that express the flowthrough or emergent velocity as a function of the impingement velocity, screen mesh, and fluid properties. Furthermore, the stability of the emerging jet was found to be dependent on the Weber number. Experiment data are compared with the developed equations and some comments are made regarding the percentage of liquid passing through the screen.

Experiment data were taken with five twilled-weave dutch screens and two test liquids (ethanol and trichlorotrifluoroethane) over a range of impingement velocities from 80 to 950 cm/sec. All data were obtained in the Lewis Research Center's 2.2-Second Drop Tower Facility, which is described in appendix A.

2

The work described herein was conducted in the U.S. customary system of units. Values were converted to the SI system for reporting purposes.

ANALYSIS OF JET-SCREEN IMPINGEMENT

The extremely complex geometry of the screens used in this study precludes any exact solutions to the equations of motion. Instead, the problem may be treated approximately, at least for the case of a circular jet impinging normally on the surface of a screen, by applying the integral momentum equation surrounding the region of interest. The control volume for this problem is shown in the following sketch:
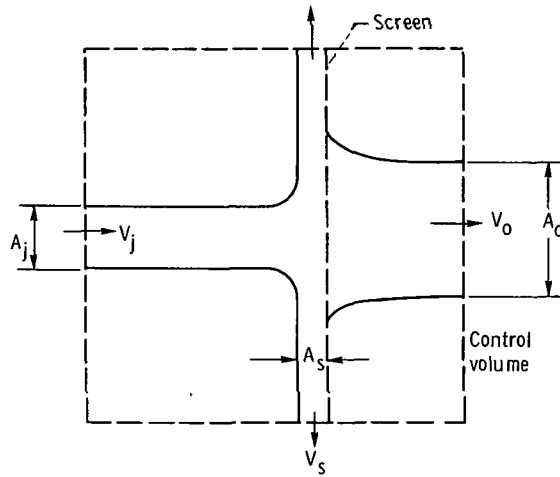
The general integral momentum equation for a control volume fixed in inertial space may be given as

$$\vec{F}_s + \iiint\limits_{cv} \vec{B}\rho \, dv = \oiint\limits_{cs} \vec{V}(\rho\vec{V} \cdot d\vec{A}) + \frac{\partial}{\partial t}\iiint\limits_{cv} \vec{V}(\rho \, dv) \tag{1}$$

(All symbols are defined in appendix B.) This equation simply relates the sum of the forces to the efflux of momentum across the control surface plus the rate of change of momentum within the control volume. For the chosen control volume, assuming steady state and zero gravity, equation (1) may be simplified to

$$\vec{F}_s = \rho A_j V_j^2 - \rho A_o V_o^2 \tag{2}$$

It is assumed that the remaining momentum equations are identically satisfied because of the symmetry of the problem.

The force on the screen is primarily due to the sum of both the viscous and inertial resistances of the screen to the passage of flow. A previously developed model (ref. 1) found that the pressure drop across woven screens could be characterized by an equation of the form

$$\Delta P_f = \frac{f \rho V^2 Q b}{\epsilon^2 D} \tag{3}$$

where

$$f = \frac{\alpha}{Re} + \beta \tag{4}$$

Substitution of equation (4) into equation (3) yields

$$\Delta P_f = \frac{\alpha \rho V^2 Q b}{\epsilon^2 \, Re \, D} + \frac{\beta V^2 Q b \rho}{\epsilon^2 D} \tag{5}$$

By letting $Re = \rho V / \mu a^2 D$, equation (5) may be written as

$$\Delta P_f = \frac{\alpha \mu a^2 Q b}{\epsilon^2} V + \frac{\beta Q b \rho}{\epsilon^2 D} V^2 \tag{6}$$

Removing those terms that are dependent only upon the geometry of the screen through the substitutions

$$C_1 = \frac{\alpha a^2 Q b}{\epsilon^2}$$

and

$$C_2 = \frac{\beta Q b}{\epsilon^2 D}$$

we may express equation (6) as

$$\Delta P_f = C_1 \mu V + C_2 \rho V^2 \tag{7}$$

Note that the velocity V used in equations (3) to (7) is defined by reference 1 to be

a fluid approach velocity. Equation (7) was analytically developed and the constants empirically determined for screens that were placed across conduits or tubes. Therefore, the fluid was constrained to pass through the screen, and the velocities on both the upstream and downstream sides of the screen were identical because of continuity requirements. In the reference 1 study, the actual velocity used in correlating the data was an average velocity determined by dividing the flow rate by the cross section of the channel.

In the problem under consideration in this study, not all of the liquid was constrained to pass through the screen since some could be deflected by the screen and, thus, flow along it. It would, therefore, not be appropriate to use the jet impingement velocity in equation (7). Rigorously, one suspects that the appropriate velocity to use in equation (7) for this problem would be an average value, possibly obtained by integrating the local axial velocity just upstream of the screen over the effective flow-through area. Unfortunately, the local upstream velocity could not be measured. However, physical intuition suggests that the average approach velocity that was used in previous studies could be represented, at least from an order-of-magnitude point of view, by the emerging-jet tip velocity V_o on the downstream side of the screen, which can be measured. Assuming that a functional relation exists between the emerging jet velocity and the pressure drop through the screen, therefore, we may write

$$\Delta P_f = F\left(C_1 \mu V_o + C_2 \rho V_o^2\right) \tag{8}$$

The force exerted on the screen then, as determined from the expression for the pressure drop, may be given as

$$A_t \, \Delta P_f = \vec{F}_s = F\left(C_1 \mu V_o + C_2 \rho V_o^2\right) A_t \tag{9}$$

By combining equations (2) and (9) we obtain

$$F\left(C_1 \mu V_o + C_2 \rho V_o^2\right) A_t = \rho A_j V_j^2 - \rho A_o V_o^2 \tag{10}$$

It is expected that A_t, the area of the screen surface through which liquid flows, will be approximately equal to A_o, the area of the emerging liquid jet. If we further assume that the area of the emerging jet is proportional to the area of the impinging jet (i.e., $A_o = KA_j$), we may rewrite equation (10) as

$$F\left(C_1 \mu V_o + C_2 \rho V_o^2\right) K = \rho V_j^2 - \rho K V_o^2 \tag{11}$$

Simplifying yields

$$K(FC_2 + 1)V_o^2 + KFC_1\left(\frac{\mu}{\rho}\right)V_o - V_j^2 = 0 \tag{12}$$

The velocity on the downstream side of the screen may be given as

$$V_o = \frac{-FKC_1\left(\frac{\mu}{\rho}\right) + \sqrt{F^2K^2C_1^2\left(\frac{\mu}{\rho}\right)^2 + 4K(FC_2 + 1)V_j^2}}{2K(FC_2 + 1)} \tag{13}$$

By using equation (13) it is then possible to determine the percentage of liquid passing through the screen as a function of the screen geometric parameters, impingement velocity, and empirically determined constants:

$$\frac{\text{Percentage of throughflow}}{100} = \frac{-FKC_1\left(\frac{\mu}{\rho}\right) + \sqrt{\left[FKC_1\left(\frac{\mu}{\rho}\right)\right]^2 + 4K(FC_2 + 1)V_j^2}}{2(FC_2 + 1)V_j} \tag{14}$$

Appropriate values of the screen geometric parameters (C_1 and C_2) can be determined from references 2 and 3 and are presented in table I. The validity of the assumptions concerning the terms K and F must now be assessed from experimental data.

APPARATUS AND TEST PROCEDURE

Test Liquids and Screen Samples

The two test liquids used in this study were ethanol and trichlorotrifluoroethane. Their properties pertinent to this investigation are presented in table II. Both liquids exhibited a near-zero static contact angle on stainless steel (the screen material), thus simulating the contact angle of typical propellants on the screen material.

Five different twilled-weave dutch meshes were tested: 200×600, 80×700, 165×800, 200×1400, and 325×2300. Samples of each screen were cut in sections approximately 10 cm (4 in.) in diameter and were clamped between two annular disks having outer diameters of 10 cm (4 in.) and inner diameters of 7.6 cm (3 in.). The sample was supported by a single threaded rod and could be positioned at any desired distance from the nozzle exit (fig. 1). In those tests reported in this study, the distance was maintained constant at 4.45 cm (1.75 in.).

6

The experiment drop package used in this study is shown in figure 1. The package was a self-contained unit consisting of the screen sample, a liquid pumping system, a photographic system, a digital clock, and an electrical system to operate the various electrical components. The liquid pumping system (shown schematically in fig. 2) consisted of two cylindrical pressure vessels 11.7 cm (4.6 in.) in diameter and 76 cm (30 in.) long that could be pressurized with filtered gaseous nitrogen, a liquid supply tank, a solenoid valve, and a liquid reservoir that terminated in a converging nozzle 0.64 cm (0.25 in.) in diameter. The shape of the nozzle was dictated by the desire to have a nearly uniform velocity diameter. Surrounding the reservoir and the screen sample was an optically clear, square, plastic enclosure 20 cm by 20 cm (8 in. by 8 in.) that was 20 cm (8 in.) deep and had side walls 1/2 cm (3/16 in.) thick. A cover plate for this enclosure was formed from two sections of plastic sheet 0.32 cm (1/8 in.) thick, 20 cm (8 in.) long, and 10 cm (4 in.) wide. This enclosure was necessary to contain the impinging liquid. To obtain a clear view of the upper surface of the screen, it was also necessary to include a liquid deflector at the outermost portion of the lower screen surface. This deflector prevented the impingement of deflected liquid onto the forward wall of the enclosure, since this liquid would obscure the required view.

The photographic system consisted of a backlighting system to provide indirect illumination of the screen sample and a high-speed 16-mm camera to record the behavior of the liquid jet during impingement on the screen surface. Time during weightlessness was observed by reading a digital clock with an accuracy of ±0.01 second that was positioned in the field of view of the camera. The clock, solenoid valve, lights, camera, and all other electrical components received their power from rechargeable nickel/cadmium batteries carried onboard.

Test Procedure

Prior to assembly of the flow components, the tanks and all lines that would contact the test liquid were cleaned in an ultrasonic cleaner to assure that the properties of the test liquids would not be affected by contaminants. Additionally, the screen samples were initially immersed in a filtered nitric acid solution at room temperature for 10 minutes, thoroughly flushed with filtered deionized water, and dried in a warm-air dryer. Each sample was then flushed in both directions with filtered methanol, rinsed again with filtered deionized water, and dried in the warm-air dryer. All parts were then assembled and mounted in the experiment drop package.

All flow lines were filled with the test liquid and activated several times to remove

any air that may have been trapped in the lines. The system was then checked for leaks. Normal-gravity calibration runs were conducted to set the desired flow rate (and, hence, the desired velocity); and two timers located in the electrical control box were adjusted. These timers set the time at which flow would be initiated and also the duration of the pumping. In the normal-gravity calibration runs, the flow rate was determined by measuring the volumetric flow rate out of the liquid supply tank and reading the time on the digital clock. A series of runs was made at each supply tank pressure to assure repeatability of the data. At the ranges of supply pressures used in this study (nominally 1.4×10^5 to 1.52×10^6 N/cm^2 (2 to 22 psig)), the effect of gravitational head was negligible and, hence, the flow rates in normal gravity and in weightlessness were assumed to be identical.

The desired quantity of test liquid was then placed in the liquid supply tank, and the required pressure was set in the supply pressure bottles. The camera was loaded, and the experiment package was balanced about its horizontal axes and positioned in the prebalanced drag shield.

RESULTS AND DISCUSSION

Liquid Behavior Following Jet Impingement

At relatively low impingement velocities, very little of the impinging liquid penetrated the screen. Any liquid that did flow through the screen tended either to puddle or to form a small geyser that either remained at the same height or decreased in height with respect to the screen surface. Examples of this type of postimpingement behavior are shown in figures 3(a) and (b) for impingement velocities of 286 and 125 cm/sec, respectively. It is apparent that the vast majority of the impinging liquid in these tests was deflected by the screen. This type of behavior following liquid impingement was also apparent in settling tests described in reference 4, where it was observed that "liquid penetration through the screen at impact was much less than expected in all cases. Liquid initially impacting the screen penetrated slightly, but it appears that most of the liquid is deflected by the screen, flows along the screen and, thus, wets it."

At higher impingement velocities, more of the impinging jet penetrates the screen. In these tests (examples of which are depicted in figs. 3(a) to (c) for impingement velocities of 362, 170, and 286 cm/sec, respectively), the impinging jet penetrated and formed a geyser that continued to grow in time with respect to the screen surface. However, it is obvious from the figure that even in those tests a considerable percentage of the impinging jet was deflected by the screen.

8

Determination of Proportionality Constant

To make the equations presented in the analysis section tractable and to formulate them in terms of initial jet parameters, it was necessary to assume that the ratio of the cross-sectional area of the emerging jet to that of the impinging jet K was a constant. Measurements of the emerging-jet cross section were made from the photographic data for those tests in which the jet formed a geyser that progressed to the top of the test tank. The results are summarized in table III. In general, the emerging jet appeared to be slightly larger in the trichlorotrifluoroethane tests for a given screen than it was in the ethanol tests, but no clear effect of either impingement velocity or screen texture was ascertained. Furthermore, the overall variation in diameter ratio for all tests was $1.81 < D_0/D_j < 2.36$, for an arithmetic average of 2. Thus, the assumption regarding K appears valid, and the average value assumed for the proportionality constant is 4 for the data herein.

Emergent Velocity

The empirically determined value of K (the proportionality constant) was used to modify equation (13) to read

$$V_o = \frac{-FC_1\left(\frac{\mu}{\rho}\right) + \sqrt{\left[FC_1\left(\frac{\mu}{\rho}\right)\right]^2 + (FC_2 + 1)V_j^2}}{2(FC_2 + 1)} \qquad (15)$$

To compare equation (15) with the experiment data, measurements of the emergent velocities were made for those runs in which the geyser progressed to the top of the test tank. In each of these runs the emerging jet velocity was very nearly constant with time. Results showing the velocity of the emerging jet flow as a function of impingement velocity for various screen-liquid combinations are presented in figure 4. In general, the emerging jet velocities were found to be at least an order of magnitude lower than the impingement velocities. Furthermore, in analyzing the data it was determined that if the term F was chosen to be constant and equal to 2, equation (15) predicted emergent velocities that were reasonably close to those actually obtained, within about ±15 percent.

By making use of equation (14) with $F = 2$ and $K = 4$, it was possible to determine what percentage of the incident liquid should be expected to pass through the screen. Over the range of impingement velocities in this study, the percentages of liquid expected to flow through the screen varied from about 4 to 14 for ethanol and about 5 to 28 for trichlorotrifluoroethane. These values are calculated, not measured, and include all data, not merely that presented in table III.

Weber Number Criterion

Previous studies by the author (refs. 5 to 8) have shown that the Weber number (the ratio of inertia to surface tension) is useful in predicting the stability of the liquid-vapor interface during inflow. In those studies, a stable interface was characterized by the formation of a geyser that either remained at the same height or decreased in height with respect to the lowest point on the liquid-vapor interface; and the unstable region was characterized by the formation of a geyser that continued to grow in height with respect to the lowest point on the liquid-vapor interface. With this in mind, an attempt was made to predict a critical impingement velocity that would cause the impinging jet to penetrate the screen and to form a geyser that grows in time with respect to the screen surface. To this end we may begin by solving equation (12) for the jet velocity V_j:

$$V_j^2 = K(FC_2 + 1)V_o^2 + KFC_1\left(\frac{\mu}{\rho}\right)V_o \tag{12}$$

Using the form of the Weber number for geyser stability from reference 8 then yields

$$We = 1.5 = \frac{V_o^2 R_o}{2\beta} = \frac{V_o^2 R_o \rho}{2\sigma} \tag{16}$$

Substitution of equation (16) into equation (12) gives

$$V_j^2 = K(FC_2 + 1)\left(\frac{3\sigma}{R_o\rho}\right) + KFC_1\left(\frac{\mu}{\rho}\right)\left(\frac{3\sigma}{R_o\rho}\right)^{1/2} \tag{17}$$

but from data, $R_o^2 = 4R_j^2$, or $K = 4$ and $F = 2$. Therefore, we may rewrite equation (17) as

$$V_j^2 = 4(2C_2 + 1)\left(\frac{1.5\,\sigma}{R_j\rho}\right) + 8C_1\left(\frac{\mu}{\rho}\right)\left(\frac{1.5\,\sigma}{R_j\rho}\right)^{1/2} \tag{18}$$

Equation (18) should then predict the critical impingement velocity that will cause the impinging liquid jet to penetrate the screen and to form a geyser that continues to grow with respect to the screen surface. Figure 5 compares the experiment data with equation (18). The solid symbols denote the tests in which the emerging jet continued to grow; the open symbols denote the tests where the emerging jet did not continue to grow. If we consider the dependence of the critical impingement velocity on several previously determined empirical constants (C_1, C_2, F, K, and We), the agreement is generally quite good.

CONCLUSIONS

An investigation was conducted to examine the gross liquid behavior of a circular liquid jet impinging onto and interacting with a simply supported, fine-mesh screen in a weightless environment. The shape of the nozzle from which the liquid jet exited was configured so as to impart a fairly uniform velocity profile to the impinging jet. The distance from the nozzle to the screen surface was maintained at 4.45 cm (1.75 in.). The impinging jet diameter was a constant 0.64 cm (0.25 in.). Two test liquids were employed, trichlorotrifluoroethane and ethanol. Five different twilled-weave meshes (200×600, 80×700, 165×800, 200×1400, and 325×2300) were tested over a range of jet impingement velocities from 80 to 950 cm/sec.

Equations were developed that expressed the flowthrough velocity as a function of the impingement velocity, liquid properties, and several empirical constants. The developed equations were compared with the data. The following conclusions were drawn:

1. By selecting appropriate values for various constants that appeared in the developed equations, those equations could be used to adequately predict (within ±15 percent) the emergent velocity downstream of the screen surface.

2. Liquid velocities downstream of the screen were at least one order of magnitude lower than the impingement velocities.

3. The diameter of the emerging jet on the downstream side of the screen was found to be approximately twice as large as the impinging jet diameter. Hence, flow through the screen occurred over an area approximately four times as large as the cross-sectional area of the impinging jet.

4. The stability of the emerging jet was shown to be Weber number dependent, with the value of the critical Weber number being 1.5.

5. The percentage of incident liquid passing through the screen was calculated to be less than 15 for all ethanol tests and less than 28 for all trichlorotrifluoroethane tests over the ranges of parameters in this study.

Lewis Research Center,
   National Aeronautics and Space Administration,
      Cleveland, Ohio, April 20, 1976,
         506-21.

APPENDIX A

TEST FACILITY

The zero-gravity data for this study were obtained in the Lewis Research Center's 2.2-Second Drop Tower Facility. A schematic diagram of the facility is shown in figure 6. The facility consists of a building 6.4 meters (21 ft) square by 30.5 meters (100 ft) tall. Contained within this building is a drop area 27 meters (89 ft) long with a cross section of 1.5 meters by 2.75 meters (5 ft × 9 ft).

The service building has, as its major elements, a shop and service area, a calibration room, and a controlled-environment room. Those components of the experiment that require special handling are prepared in the controlled-environment room of the facility. This air-conditioned and filtered room contains an ultrasonic cleaning system and the laboratory equipment necessary for the handling of test liquids (fig. 7).

Mode of Operation

A 2.2-second period of weightlessness is obtained by allowing the experiment package to fall from the top of the drop area. To minimize air drag on the experiment package, it is enclosed in a drag shield that is designed with a high ratio of weight to frontal area and a low drag coefficient. The relative motion of the experiment package with respect to the drag shield during a test is shown in figure 8. During a test, the experiment package and drag shield fall freely and independently of each other; that is, no guide wires, electrical lines, and so forth, are connected to either. Therefore, the only force acting on the freely falling experiment package is the air drag associated with the relative motion of the package within the enclosure of the drag shield. This air drag results in an equivalent gravitational acceleration acting on the experiment that is estimated to be below 10^{-5} g's.

Release System

The experiment package installed within the drag shield is suspended at the top of the drop area by a highly stressed music wire that is attached to the release system. This release system consists of a double-acting air cylinder with a hard steel knife edge that is attached to the piston. Pressurization of the air cylinder drives the knife edge against the wire, which is backed by an anvil. The resulting notch causes the

wire to fail and smoothly release the experiment. No measurable disturbances are imparted to the package by this release procedure.

Recovery System

After the experiment package and drag shield have traversed the total length of the drop and have been decelerated in a 2.1-meter (7-ft) deep container filled with sand, they are recovered. The deceleration rate (average 15 g's) is controlled by selectively varying the tips of the deceleration spikes mounted on the bottom of the drag shield (fig. 8). When the drag shield impacts in the deceleration container, the experiment package has traversed the vertical distance within the drag shield (compare figs. 8(a) and (c)).

SYMBOLS

A	area, cm^2
A_j	cross section of impinging jet, cm^2
A_o	cross section of emerging jet, cm^2
A_s	cross section of radial flow parallel to screen surface, cm^2
A_t	area of screen through which flow takes place, cm^2
a	surface area to unit volume ratio of screen wire, cm^{-1}
B	force per unit mass, N/g
b	thickness of screen, cm
C_1	screen geometrical constant, cm^{-1}
C_2	screen geometrical constant
D	screen pore diameter, cm
D_j	impinging jet diameter, cm
D_o	emerging jet diameter
d	differential
F	constant
F_s	force, N
f	friction factor
K	proportionality constant, A_o/A_j
ΔP_f	frictional pressure drop, N/cm^2
Q	tortuosity factor
R_j	radius of impinging jet, cm
R_o	radius of emerging jet, cm
Re	Reynolds number
V	velocity, cm/sec

V_j	velocity of impinging jet, cm/sec
V_o	velocity of emerging jet, cm/sec
V_s	velocity of radial flow along screen, cm/sec
We	Weber number
α	viscous resistance coefficient
β	inertial resistance coefficient
ϵ	screen-volume void fraction
μ	liquid viscosity, g/(cm)(sec)
ν	volume
ρ	density of liquid, g/cm^3
σ	surface tension, N/cm

Subscripts:

| cs | control surface |
| cv | control volume |

Superscript:

| $\rightarrow$ | vector quantity |

REFERENCES

1. Armour, James C.; and Cannon, Joseph N.: Fluid Flow Through Woven Screens. A.I.Ch.E. J., vol. 14, no. 3, May 1968, pp. 415-420.

2. Blatt, M. H.; Stark, J. A.; and Siden, L. E.: Low Gravity Propellant Control Using Capillary Devices in Large Scale Cryogenic Vehicles, Phase 1. (GDC-DDB 70-006, General Dynamics/Convair; NAS8-21465) NASA CR-102900, 1970.

3. Cady, E. C.: Study of Thermodynamic Vent and Screen Baffle Integration for Orbital Storage and Transfer of Liquid Hydrogen. (MDC-G4798, McDonnell-Douglas Astronautics Co.; NAS3-15846) NASA CR-134482, 1973.

4. Burge, G. W.; and Blackmon, J. B.: Study and Design of Cryogenic Propellant Acquisition Systems. Volume 2: Supporting Experimental Program. (MDC-G5038-Vol-2, McDonnell Douglas Astronautics Co.; NAS8-27685) NASA CR-120301, 1973.

5. Symons, Eugene P.; Nussle, Ralph C.; and Abdalla, Kaleel L.: Liquid Inflow to Initially Empty Hemispherically Ended Cylinders During Weightlessness. NASA TN D-4628, 1968.

6. Symons, Eugene P.: Liquid Inflow to Partially Full, Hemispherical-Ended Cylinders During Weightlessness. NASA TM X-1934, 1969.

7. Symons, Eugene P.: Interface Stability During Liquid Inflow to Initially Empty Hemispherical Ended Cylinders in Weightlessness. NASA TM X-2003, 1970.

8. Symons, Eugene P.; and Staskus, John V.: Interface Stability During Liquid Inflow to Partially Full, Hemispherical Ended Cylinders During Weightlessness. NASA TM X-2348, 1971.

TABLE I. - SCREEN PARAMETERS

[Tortuosity factor, Q, 1.3.]

	Screen				
	325×2300	200×1400	165×800	200×600	80×700
Viscous resistance coefficient, α	3.2	4.2	3.3	6.9	5.19
Inertial resistance coefficient, β	0.19	0.2	0.17	0.3	0.2
Thickness of screen, b, cm	0.0089	0.1524	0.1753	0.015	0.0254
Screen-volume void fraction, ϵ	0.245	0.248	0.426	0.562	0.369
Screen pore diameter, D, cm	0.0005	0.001	0.0025	0.00399	0.0025
Ratio of surface area to unit volume ratio of wire screen, a, cm^{-1}	1102.35	653.9	413.6	356	318
Screen geometrical constants:					
C_1, cm^{-1}	749532	578491	70889	53989.7	127275.8
C_2	73.25	64.43	8.54	4.64	19.4

TABLE II. - LIQUID PROPERTIES AT 20° C

	Liquid	
	Ethanol	Trichlorotrifluoroethane
Surface tension, σ, N/cm	22.3×10^{-5}	18.6×10^{-5}
Density, ρ, g/cm^3	0.789	1.579
Viscosity, μ, g/(cm)(sec)	1.2×10^{-2}	0.7×10^{-2}

18

TABLE III. - VALUES OF PROPORTIONALITY CONSTANT

[Emerging jet grows in time.]

Screen	Impingement velocity, V_j, cm/sec	Test liquid	Emerging jet diameter,[a] D_o	Proportionality constant,[b] K, D_o^2/D_j^2	Emerging jet velocity, V_o, cm/sec
200×600	226	Ethanol	$2.00\ D_j$	4.00	6.17
200×600	269	Ethanol	$2.01\ D_j$	4.04	9.91
200×600	125	Trichloro-trifluoroethane	$2.15\ D_j$	4.62	3.66
165×800	286	Ethanol	$1.83\ D_j$	3.35	8.95
165×800	170	Trichloro-trifluoroethane	$1.85\ D_j$	3.42	10.83
80×700	330	Ethanol	$1.81\ D_j$	3.28	6.26
80×700	362	Ethanol	$1.83\ D_j$	3.35	7.11
80×700	210	Trichloro-trifluoroethane	$2.36\ D_j$	5.57	6.38

[a]Average $D_o \sim 2$.
[b]Average $K \sim 4$.

Electrical control box

Batteries

Screen sample

Liquid supply tank

Liquid reservoir

Backlighting

C-75-2174

Pressure bottles

Pressure gage

Clock

Camera
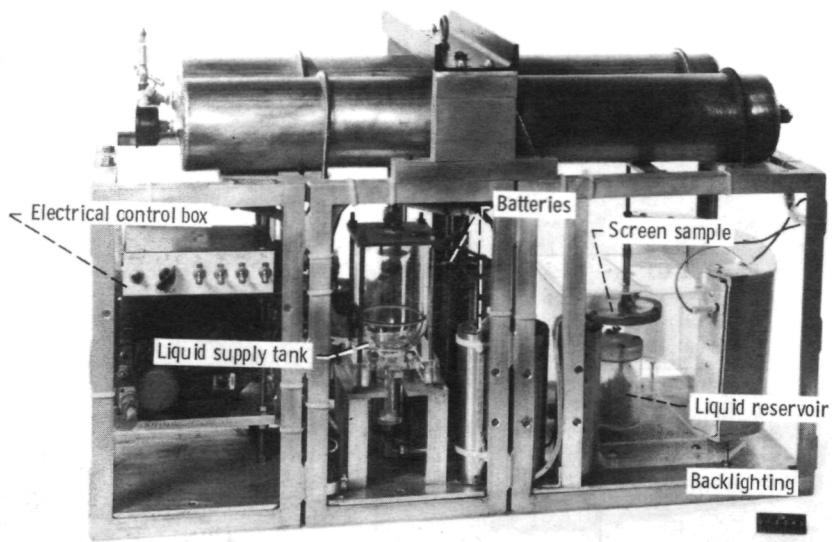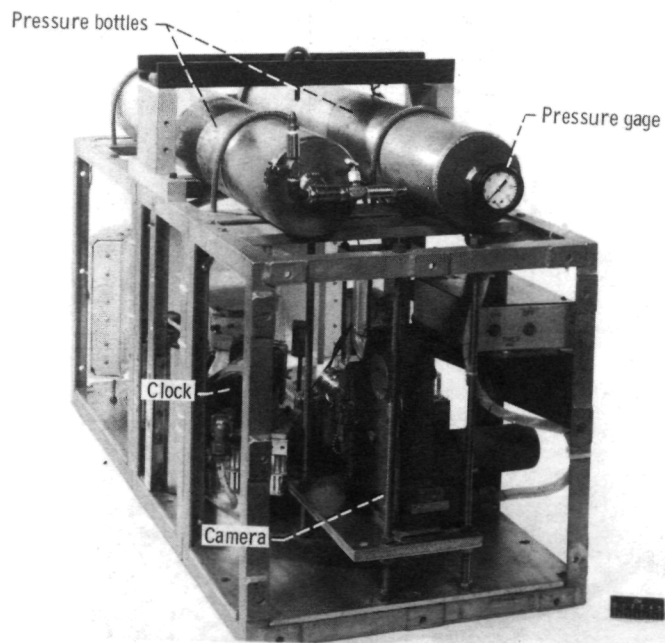
C-75-2175

Figure 1. - Experiment drop package.
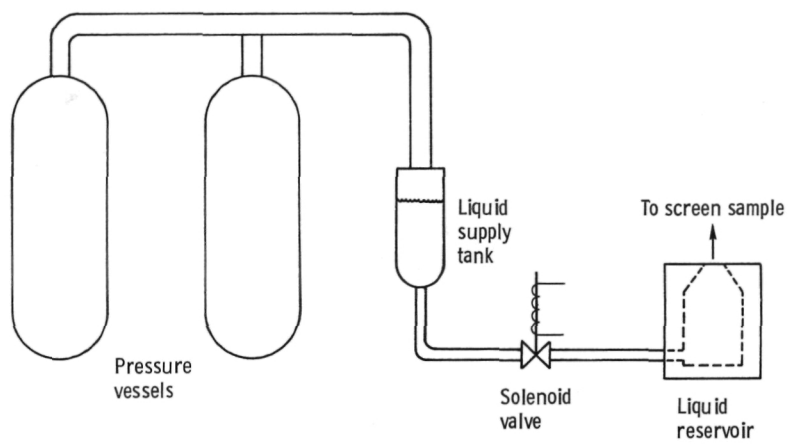
Figure 2. – Schematic of pumping system.
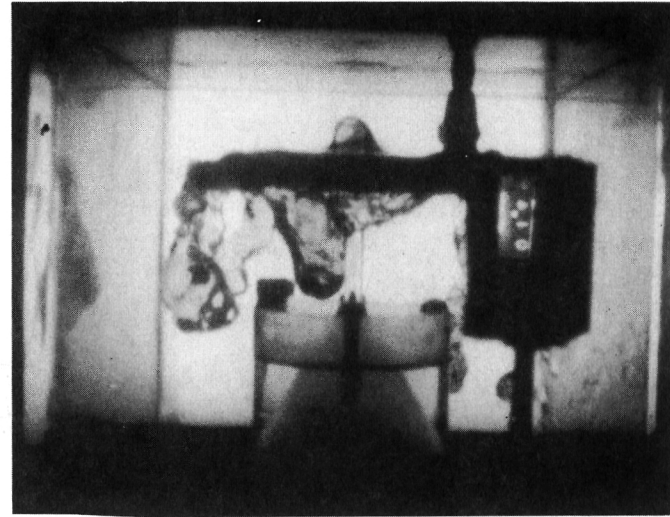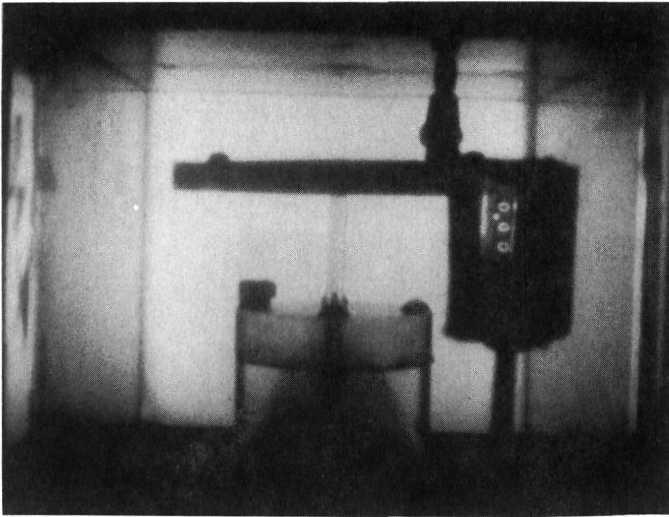
(a-1) Impingement velocity, 286 cm/sec.
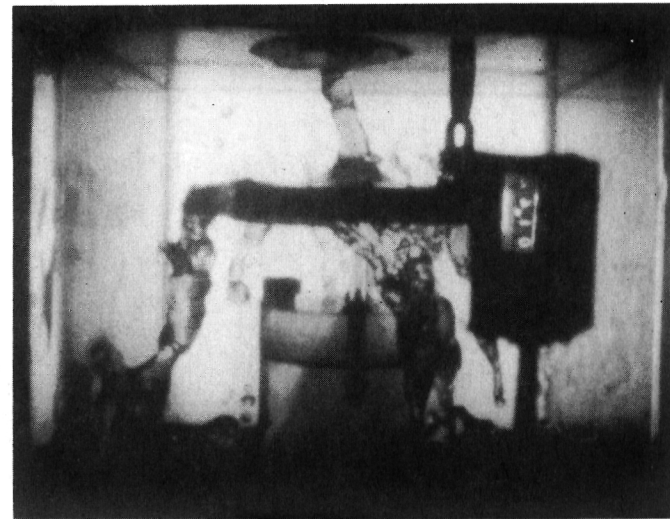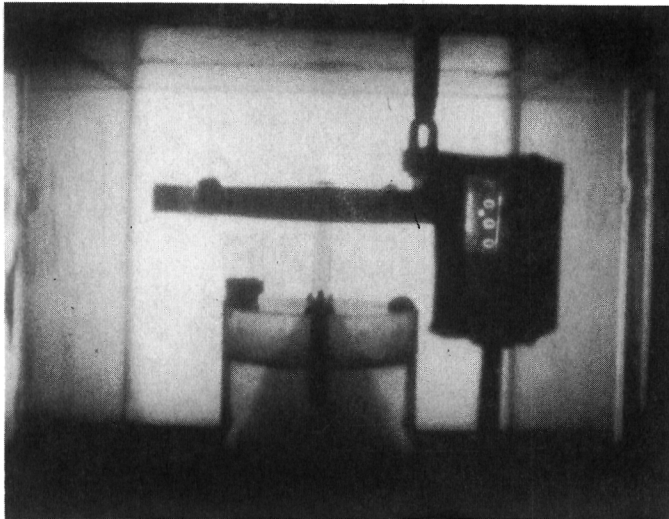
(a-2) Impingement velocity, 362 cm/sec.

(a) 80x700 Twilled-weave dutch screen; ethanol.

Figure 3. - Jet-screen impingement in weightlessness.
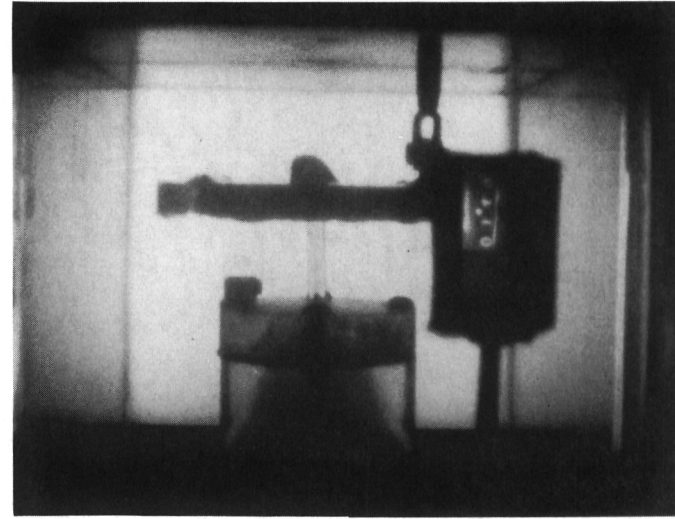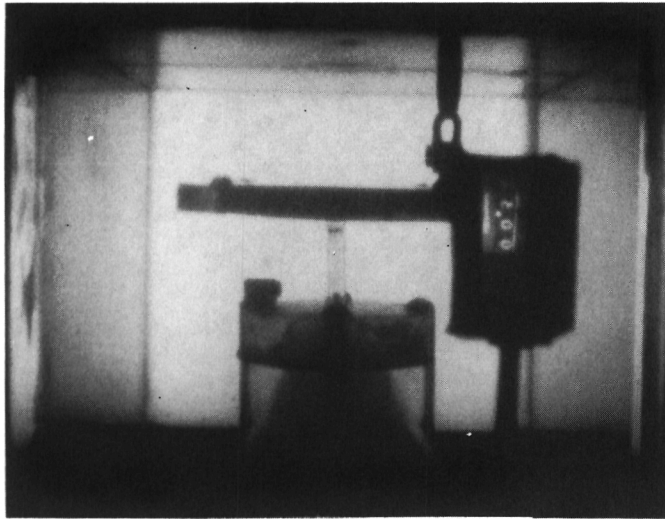
(b-1) Impingement velocity, 125 cm/sec.
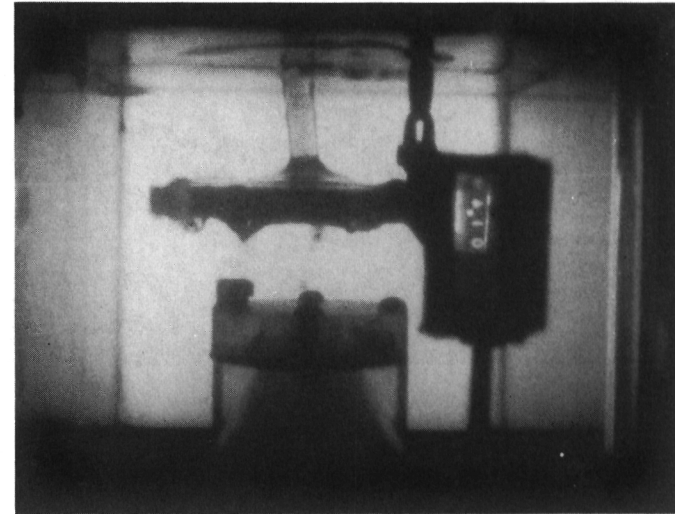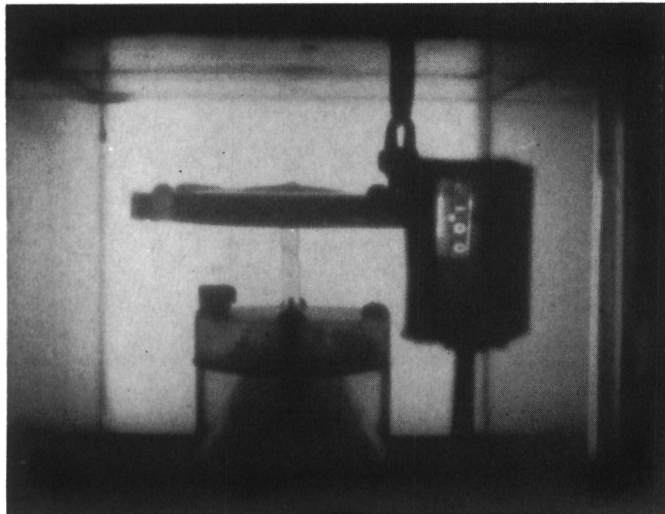
(b-2) Impingement velocity, 170 cm/sec.

(b) 165x800 Twilled-weave dutch screen; trichlorotrifluoroethane.

Figure 3. - Continued.
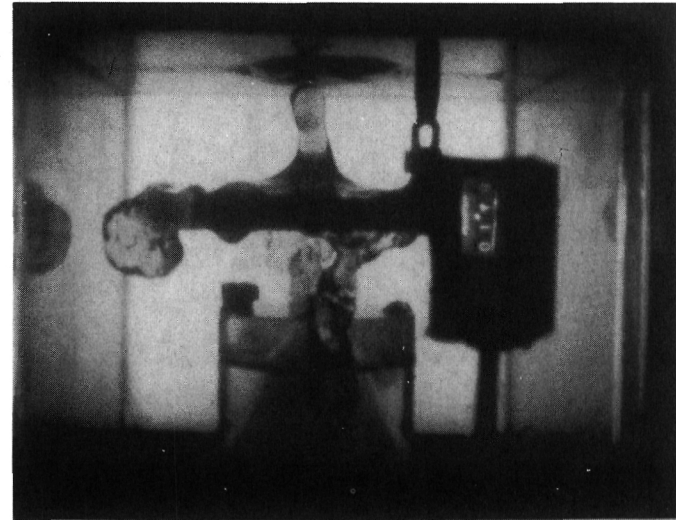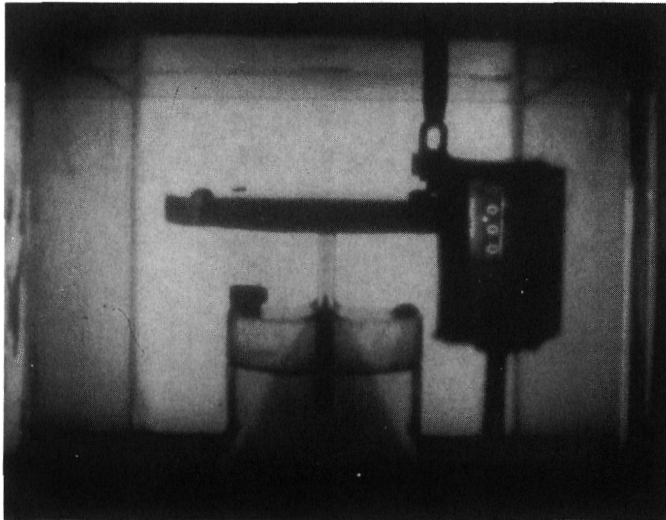
(c) 165x800 Twilled-weave dutch screen; ethanol; impingement velocity, 286 cm/sec.

Figure 3. - Concluded.
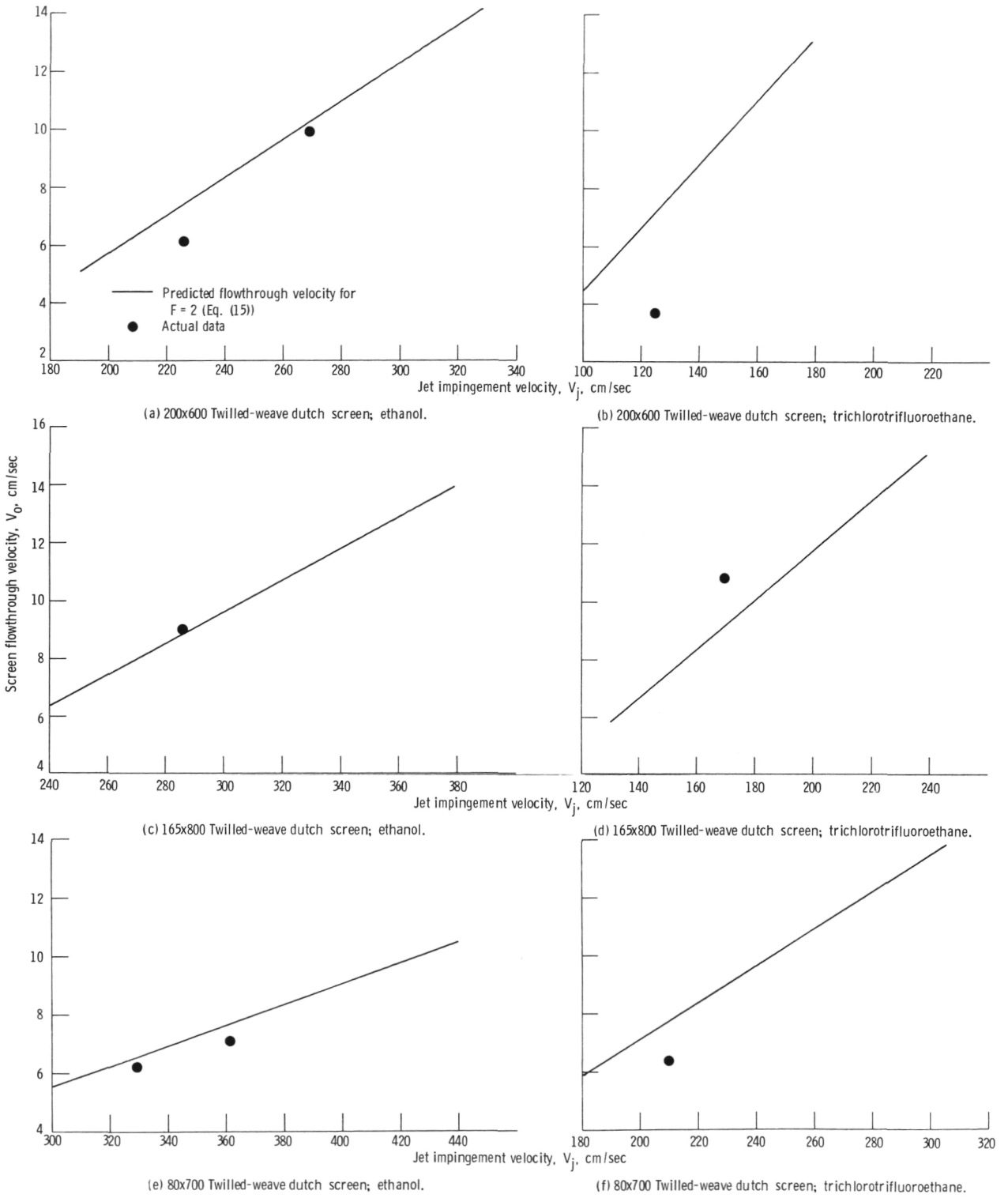
Figure 4. - Flowthrough velocity as function of impingement velocity. (Emerging jet grows in time.)
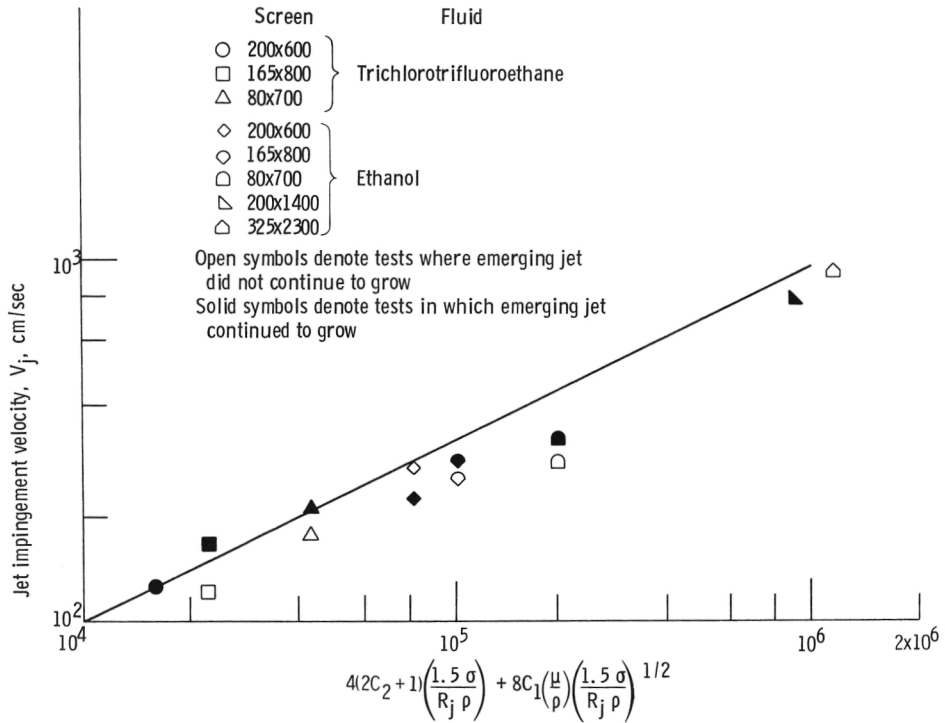
Figure 5. – Predicted critical impingement velocity compared with experiment data.

$$4(2C_2 + 1)\left(\frac{1.5\,\sigma}{R_j\,\rho}\right) + 8C_1\left(\frac{\mu}{\rho}\right)\left(\frac{1.5\,\sigma}{R_j\,\rho}\right)^{1/2}$$
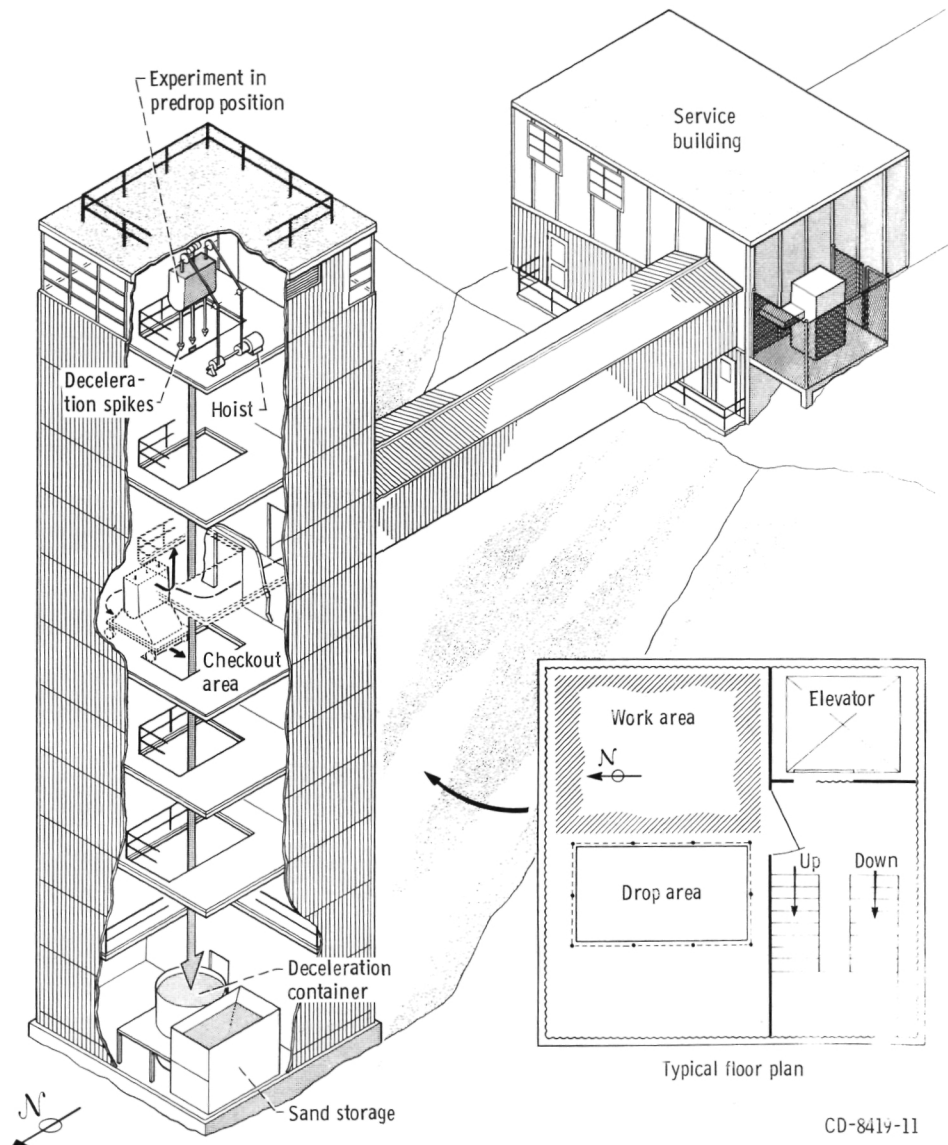
Figure 6. - 2.2-Second Drop Tower Facility.

Experiment in
predrop position

Service
building

Decelera-
tion spikes

Hoist

Checkout
area

Elevator

Work area

N

Drop area

Up   Down

Deceleration
container

Typical floor plan

Sand storage

CD-8419-11

27
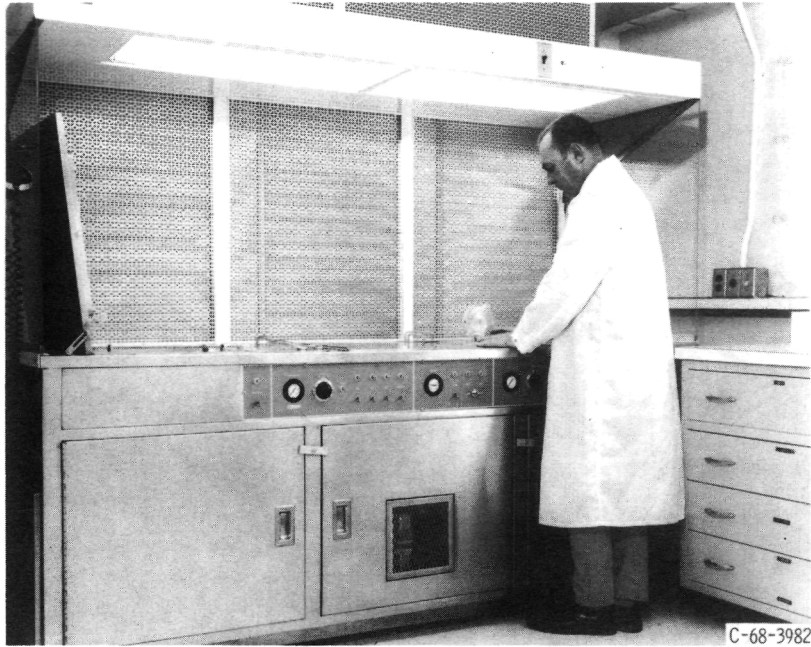
(a) Ultrasonic cleaning system.
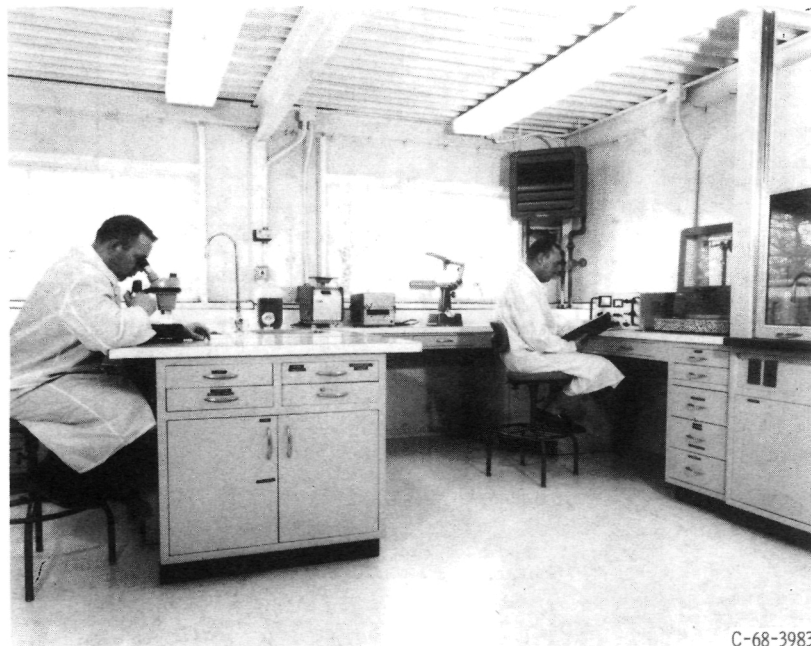
(b) Laboratory equipment.

Figure 7. - Controlled-environment room.

Double-acting piston

Anvil

Music-wire support

Wire-release mechanism

Access hole

Experiment package

Drag shield

Base rounded to reduce air drag

(a) Before release.

(b) During free fall.

(c) After deceleration.
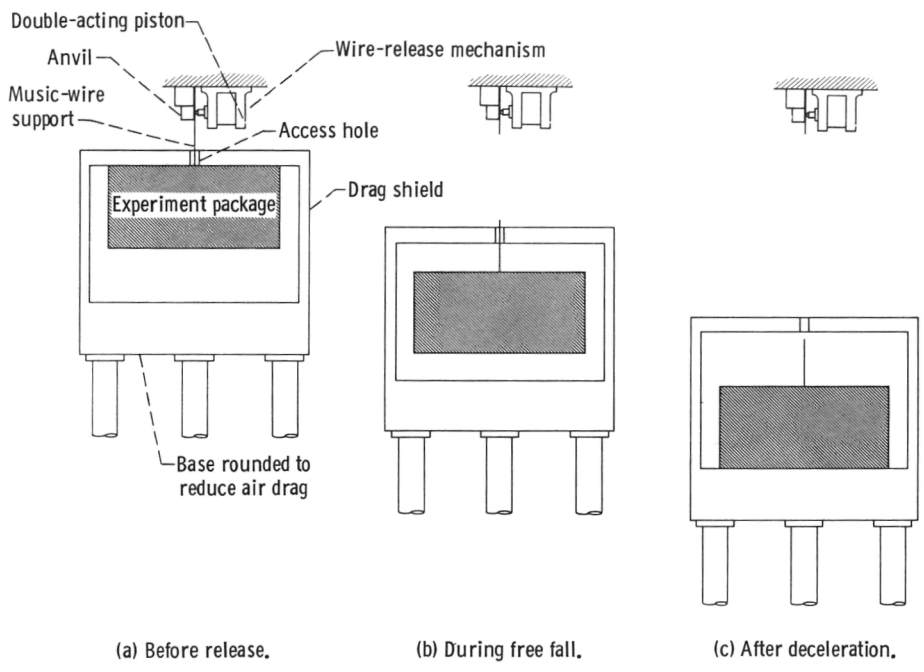
CD-7380-13

Figure 8. – Position of experiment package and drag shield before, during, and after test drop.